Holocene monsoonal dynamics and fluvial terrace formation in the northwest Himalaya, India

B. Bookhagen* Institut für Geowissenschaften, Universität Potsdam, 14415 Potsdam, Germany
D. Fleitmann Geological and Environmental Sciences, Stanford University, Stanford, California 94305, USA
K. Nishiizumi Space Sciences Laboratory, University of California, Berkeley, California 94720, USA
M.R. Strecker, R.C. Thiede Institut für Geowissenschaften, Universität Potsdam, 14415 Potsdam, Germany

ABSTRACT

Aluminum-26 and beryllium-10 surface exposure dating on cut-and-fill river-terrace surfaces from the lower Sutlej Valley (northwest Himalaya) documents the close link between Indian Summer Monsoon (ISM) oscillations and intervals of enhanced fluvial incision. During the early Holocene ISM optimum, precipitation was enhanced and reached far into the internal parts of the orogen. The amplified sediment flux from these usually dry but glaciated areas caused alluviation of downstream valleys up to 120 m above present grade at ca. 9.9 k.y. B.P. Terrace formation (i.e., incision) in the coarse deposits occurred during century-long weak ISM phases that resulted in reduced moisture availability and most likely in lower sediment flux. Here, we suggest that the lower sediment flux during weak ISM phases allowed rivers to incise episodically into the alluvial fill.

Keywords: geomorphology, Himalaya, monsoon, fluvial processes.

INTRODUCTION

The Indian Summer Monsoon (ISM) exerts a profound control on erosional hillslope processes, river discharge, and sediment flux along the southern Himalayan front (e.g., Bookhagen et al., 2005a; Goodbred and Kuehl, 2000). Numerous Holocene paleoclimate records reveal large fluctuations in the intensity and spatial extent of the ISM (e.g., Fleitmann et al., 2003; Gasse et al., 1991; Gupta et al., 2003; Thompson et al., 2000). The effect of these changes on the fluvial transport system remains unclear. Here, we focus on the erosional impact of recently documented ISM drought events (10^2–10^3 yr) that are in detail constrained through stalagmite $\delta^{18}O$ records (e.g., Fleitmann et al., 2003; Dykoski et al., 2005; Wang et al., 2005) and pollen data in lacustrine sediments on the Tibetan Plateau (e.g., Gasse et al., 1991; Van Campo et al., 1996). While the ISM during the early to middle Holocene was overall stronger than today, several century-long intervals of reduced rainfall and moisture migration, such as at 8.5, 6.4, and 2.7 k.y. B.P., can be detected in numerous ISM records (e.g., Fleitmann et al., 2003; Gasse et al., 1991; Van Campo et al., 1996; Wang et al., 2005). These climate archives and present-day meteorological observations in the Himalayan realm demonstrate that fluctuations in ISM intensity influenced moisture migration on the Tibetan Plateau, and thereby strongly affected sediment flux in large river systems (e.g., Bookhagen et al., 2005b; Goodbred and Kuehl, 2000; Pratt-Sitaula et al., 2004).

In order to understand the fluvial response to large-scale, catchment-wide ($\sim 50 \times 10^3$ km^2) climatic fluctuations, we analyzed fluvial terraces near the outlet of the Sutlej River (77.5°N, 31.45°W) on the southern flank of the Himalaya orogen. There, downcutting of an early Holocene conglomeratic valley fill occurred episodically involving six ~10–30 m steps. Although dating of the heavily weathered, densely vegetated, and partially anthropogenically influenced terraces is a challenge, we were able to construct a consistent terrace chronology in a dry, well-preserved and less-altered part of the lower Sutlej River. This chronology is based on both ^{26}Al and ^{10}Be surface exposure ages and radiocarbon dating. The coincidence between weak (dry) ISM intervals and the cutting of terraces in the fill unit suggests that terrace formation is linked to lower sediment flux during these intervals. We infer that the resultant decreased ratio between fluvial sediment flux and transport capacity promoted incision and terrace formation.

SETTING, METHODS, AND APPROACH

A massive conglomeratic fill occupies the lower Sutlej Valley south of Rampur over a distance of ~80 km, immediately downstream of the narrow, high-gradient river gorge (Fig. 1). The highest terrace (labeled T1 in Fig. 2) in a sequence of six surfaces near Rampur is 120 m above the present stream, and terrace heights (T2 to T6) decrease downstream. The terraces comprise large boulders and gravels, indicating high-energy, braided-stream characteristics. We do not observe a change in grain sizes or depositional environment in this deposit, indicative for a steady and fast alluviation event. The clast provenance primarily reflects the upstream, internal parts of the catchment, where lithologies of the Higher Himalayan Crystalline and Tethyan Sediment Series dominate. We surveyed these terraces using a differential GPS and determined their exposure ages with cosmogenic radionuclides (^{10}Be: $T_{1/2} = 1.5 \times 10^6$ yr, ^{26}Al: $T_{1/2} = 7.05 \times 10^6$ yr) on conglomeratic clasts collected on the terrace surfaces. These ages define abrupt terrace abandonment as fluvial incision occurred. A crucial factor in dating boulders and pebbles from alluvial surfaces with cosmogenic nuclides is radionuclide inheritance, as prior exposure of pebbles during exhumation and/or transport might significantly alter nuclide concentration and ultimately leads to wrong age estimations (e.g., Anderson et al., 1996; Repka et al., 1997). In order to account for pebble-specific exposure history, we collected a total of 30–40 quartz-rich clasts (2–5 cm in diameter) from each terrace. In addition, we collected samples (BB2 and BB11) from single, large, granitic boulders (3–4 m in diameter) with distinct fluvial erosion marks (e.g., potholes). Furthermore, to estimate cosmogenic inheritance, four samples were collected from a 2 m deep profile (BB3 to BB7). Each of these samples consists of ~35 quartz-rich clasts with composition similar to the surface samples.

The depth samples agree with the theoretical cosmogenic nuclide concentration (Fig. 3), indicating that there was no initial or only negligible predepositional radionuclide content and no erosion or redeposition event after terrace formation. We thus infer pristine, in situ terrace surfaces, an assessment that is further corroborated by the following field observations: (1) There is no evidence of bioturbation within the gravels; (2) original depositional imbrication is still intact; (3) surface clasts do not display carbonate coatings,

*E-mail: bodo@crustal.ucsb.edu; Current address: Institute for Crustal Studies, University of California–Santa Barbara, Santa Barbara, California 93106, USA.

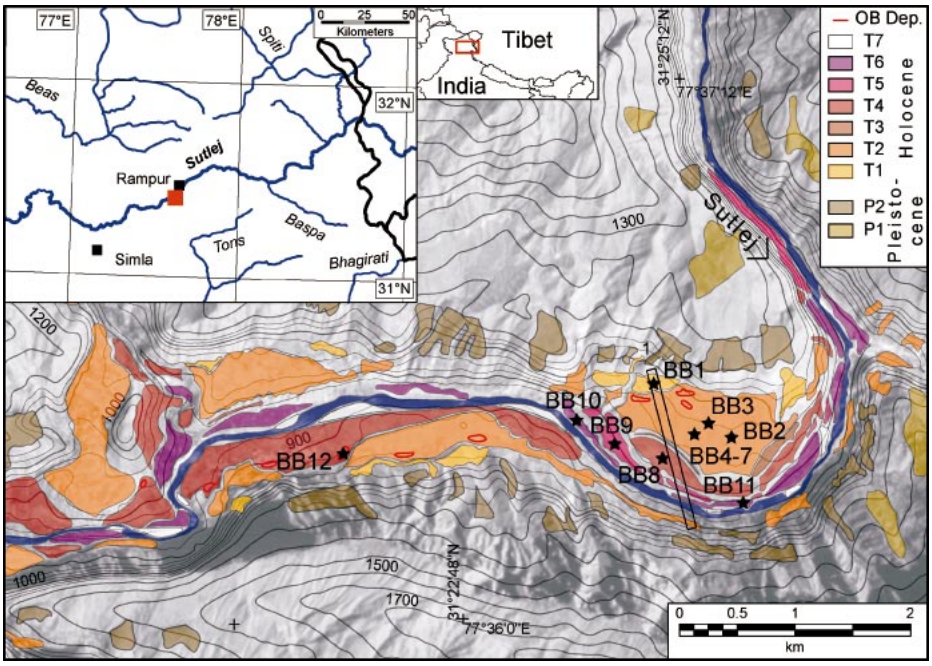

Figure 1. Detailed view of the fluvial cut-and-fill sequence in the lower Sutlej River near Rampur (orange box). Color-coded terraces were mapped in the field and draped over a Corona satellite image. Contour lines are derived from hand-digitized topographic maps. Sample locations are shown by black stars. The dominant terrace levels T2 and T4 can be followed for ~80 km farther downstream and upstream into tributaries. Red polygons indicate overbank (OB) deposits. Black box outlines topographic cross profile shown in Figure 4.

Figure 2. Photograph of the alluvial infill in the lower Sutlej Valley, taken from the eastern part of Figure 1 toward the southwest. The Sutlej River is flowing to the upper part of the picture.

and clasts with carbonate coatings are confined to the soil B-horizons; and (4) soil-profile development on the highest (oldest) surface is most pronounced, whereas profile development decreases systematically on lower, younger surfaces.

We have processed cosmogenic nuclide concentrations following standard procedures (Kohl and Nishiizumi, 1992) and calculated ages following Lal (1991) by using revised production rates of 5.1 and 31.1 atoms/g qtz for ^{10}Be and ^{26}Al, respectively (Clark et al., 1995). We corrected for geomagnetic field changes using the approach by Nishiizumi et al. (1989) with reconstructed geomagnetic poles during the Holocene (Ohno and Hamano, 1992). Topographic shielding has been measured in the field and is included in age estimations. There is no snow coverage at these elevations. All ages include 1σ analytical errors. To account for decreased production rates at depth, the ages of subsurface samples are ''depth-corrected'' with $\rho = 1.8 \pm 0.2$ g/cm^3 and $\Lambda = 160 \pm 10$ g/cm^2 (e.g., Repka et al., 1997).

To decipher the role of past ISM oscillations in changing precipitation regimes, we have used oxygen isotope ratios (δ^{18}O) measured in stalagmites from southern Oman and Dongge Cave, China (Fleitmann et al., 2003; Wang et al., 2005). Studies in Oman demonstrate that δ^{18}O values are inversely related to the amount of rainfall, primarily via an ''amount effect'' (Burns et al., 1998; Fleitmann et al., 2003). A stronger monsoon circulation increases thermal convection, enhances depletion of the lighter isotope, and thus results in lower δ^{18}O values. We have used oxygen isotope records in conjunction with the lower-resolution paleolake records from the Tibetan Plateau (Gasse et al., 1991; Gasse et al., 1996; Lister et al., 1991; Van Campo et al., 1996) to identify century-long dry events that occurred from 8.7 to 8.1, 6.6 to 6.2, and ca. 3.6 and 2.7 k.y. B.P. While the ages from the Tibetan paleolakes are controversial, it is important to note that these arid events also had a global expression reflected in cold and dry conditions in the Northern Hemisphere and the tropics (e.g., Grootes et al., 1993; Lachniet et al., 2004; Rohling and Pälike, 2005). It is therefore expected that these changes had an impact on surface processes as well.

RESULTS

We present ages averaged over both nuclides (^{26}Al and ^{10}Be), constituting two independent measurements. In general, ages from both nuclides agree very well (Table 1). The formation of the highest terrace surface (T1, 120 m above modern grade; sample BB1) coincides with the onset of the ISM in early Holocene at 9.9 ± 0.5 k.y. B.P. (Table 1). This surface is now highly dissected and forms isolated remnants along the present stream. For these deposits, the averaged alluvial incision rate is 12.1 ± 0.6 mm/yr, similar to estimates of 11 ± 8.5 mm/yr in a comparable fluvial environment in central Nepal (Pratt-Sitaula et al., 2004). The second highest and most pronounced terrace surface (T2, 110 m above modern grade; samples BB2 and BB3) was abandoned at 8.6 ± 0.4 k.y. B.P. It is contiguous upstream into large tributaries and indicates a regional response to external forcing factors, not confined to the main stem. Both amalgamated (BB2) and single-rock samples (BB3) provide a similar age. In some places, fine-grained overbank deposits cover the terrace conglomerates near the valley flanks. We interpret these deposits as remnants from flood overspills, while the channel was downcut. Only high flows would have overcome the channel tops and deposited suspended sediments on the adjacent surface. The age of T2 falls into the beginning of the period between ca. 8.7 and 8.1 k.y. B.P., which was characterized by a cold and dry, weak ISM phase (Fig. 4) (e.g., Fleitmann et al., 2003; Gasse et al., 1991; Van Campo et al., 1996; Wang et

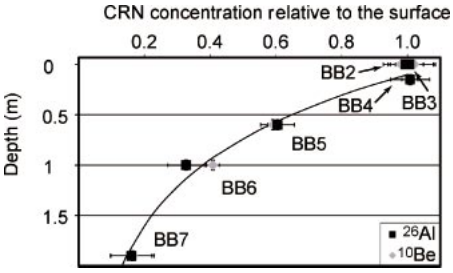

Figure 3. Depth profile on terrace level T2 to demonstrate negligible cosmogenic nuclide inheritance. Cosmogenic radionuclide (CRN) concentration is given relative to the mean of the two surface sample concentrations (BB2 and BB3), and we included muon production in the theoretical depth-profile calculations (Granger and Smith, 2000).

TABLE 1. Al AND Be CONCENTRATIONS

Sample (Terrace number-depth)	Elevation asl (m)	Height above modern Sutlej (m)	^{10}Be (10^3 atoms/g qtz)	^{10}Be age (k.y. BP)	^{26}Al (10^3 atoms/g qtz)	^{26}Al age (k.y. BP)	^{10}Be-^{26}Al Mean age (k.y.BP)
BB1 (T1-0m)	1020	120	93.7 ± 3.1	9.8 ± 0.7	578 ± 20	10.0 ± 0.7	9.9 ± 0.5
BB2 (T2-0m)	1005	105	78.1 ± 2.4	8.4 ± 0.6	494 ± 26	8.7 ± 0.7	8.5 ± 0.5
BB3 (T2-0m)	1005	105	81.4 ± 4.6	8.7 ± 0.7	489 ± 39	8.6 ± 0.9	8.7 ± 0.6
BB4 (T2-0.2m)	1005	105	80.3 ± 1.9	10.1 ± 0.6	495 ± 29	10.2 ± 0.9	10.1 ± 0.5
BB5 (T2-0.6m)	1005	105	47.1 ± 1.2	9.8 ± 0.6	297 ± 25	10.2 ± 1.1	10.0 ± 0.5
BB6 (T2-1.0m)	1005	105	32.5 ± 0.9	10.6 ± 0.7	161 ± 16	8.7 ± 1.0	9.6 ± 0.6
BB7 (T2-1.9m)	1005	105	13.1 ± 2.2	11.7 ± 2.1	79 ± 10	11.5 ± 1.7	11.6 ± 1.3
BB8 (T4-0m)	965	65	59.0 ± 2.5	6.8 ± 0.5	356 ± 17	6.8 ± 0.5	6.8 ± 0.4
BB9 (T5-0m)	920	20	27.5 ± 2.3	3.4 ± 0.3	185 ± 11	3.7 ± 0.3	3.6 ± 0.2
BB10 (T6-0m)	892	6	23.1 ± 2.2	3.0 ± 0.3	159 ± 22	3.4 ± 0.5	3.2 ± 0.3
BB11 (T6-0m)	893	7	21.1 ± 0.8	2.8 ± 0.2	134 ± 10	2.9 ± 0.3	2.8 ± 0.2

al., 2005; Rohling and Pälike, 2005). Terrace level T3 was not sampled because of the poor preservation of the small relict surfaces. However, because this terrace is bracketed by the well-dated terrace levels T2 and T4, we tentatively link level T3 with a weak ISM interval at ca. 7 k.y. B.P. (Fig. 4). The third lowest terrace, T4, is clearly distinguishable (BB8) and is 6.8 ± 0.4 k.y. old. As for T2, we have observed overbank deposits that we attribute to overspills during floods while the channel was incising near the center of the wide river valley. Pieces of charcoal found in these deposits are 6.6 ± 0.1 cal. ^{14}C k.y. old. Again, abandonment of the pronounced T4 level coincides with the beginning of a prominent weak ISM phase between ca. 6.7 and 6.1 k.y. B.P. (e.g., Fleitmann et al., 2003; Wang et al., 2005). The ISM strength generally decreased between 6.2 and 3.5 k.y. B.P. (Fig. 4), but no pronounced dry events occurred, which may explain the lack of terraces in middle Holocene time. The lower, minor level of T5 (25 m above modern grade; BB9) is 3.6 ± 0.2 k.y. old and coincides with a dry event ca. 3.6 k.y. B.P. (e.g., Fleitmann et al., 2003; Van Campo et al., 1996; Wang et al., 2005). T6 (10 m above modern grade; samples BB10 and BB11) is 3.0 ± 0.1 k.y. old and correlates with low solar activity at ca. 2.7 k.y. B.P., indicating very weak ISM intensity during the Holocene (e.g., Fleitmann et al., 2003; Dergachev et al., 2004; Wang et al., 2005). Presently, the lower Sutlej River flows partly over bedrock where it has regained the base level it had already achieved prior to the rapid alluviation in early Holocene time. Thus, in the Holocene, the lower Sutlej River experienced a rapid aggradation event during the early stages of the ISM at ca. 9.9 k.y. B.P., which was followed by stepwise incision linked to drier ISM anomalies.

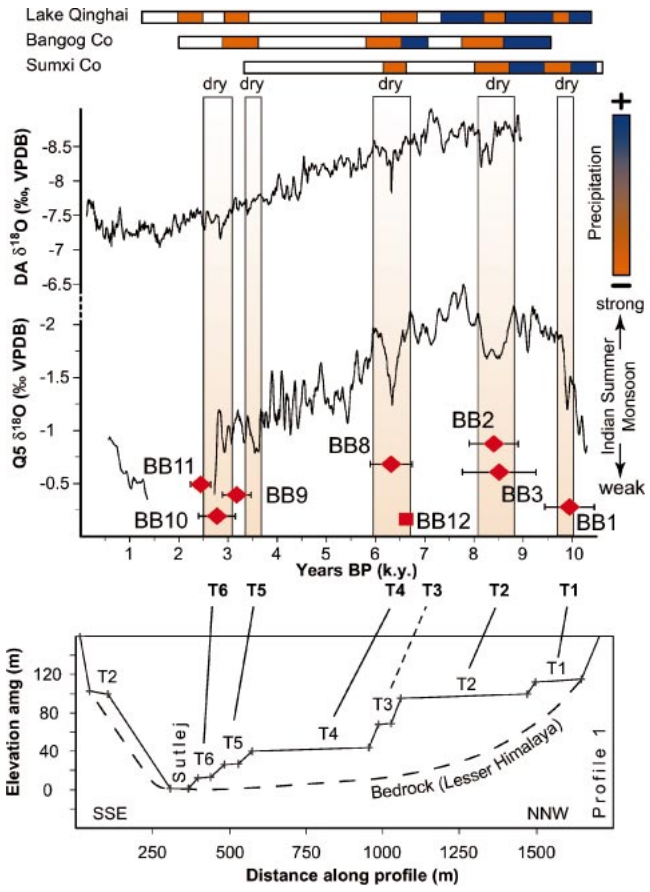

Figure 4. Holocene Indian Summer Monsoon (ISM) oscillations based on two ten-point running average δ^{18}O records from southern Oman (Q5) (Fleitmann et al., 2003) and southeast China (DA) (Wang et al., 2005). Lower δ^{18}O values indicate stronger ISM convection and higher precipitation. Lake Qinghai (Lister et al., 1991), Bangog Co (Gasse et al., 1996; Van Campo et al., 1996), and Sumxi Co (Gasse et al., 1991) are lake-sediment archives that have a millennial temporal resolution, but indicate similar moisture-migration trends onto the Tibetan Plateau ca. 8.5, 6.4, 3.2, and 2.7 k.y. B.P. Note that climate proxies indicate periods of lower moisture availability compared to previous humid phases. Red diamonds indicate averaged ^{26}Al-^{10}Be cosmogenic exposure ages (Table 1); thus each point represents two measurements. Sample BB12 is a radiocarbon sample from an overbank deposit found on level T4 that is 6.7 ± 0.06 k.y. old (Stuiver et al., 1998). Orange boxes outline dry phase extent to show overlap with terrace-abandonment ages. Location for terrace profile 1 is given on Figure 1; note profile reversal that now runs from south to north. Terrace levels are labeled T1 to T6 amg—above modern grade.

DISCUSSION AND CONCLUSION

Distinct dry intervals spike the overall stronger than today ISM between ca. 10 and ca. 2 k.y. B.P. (e.g., Fleitmann et al., 2003; Gasse et al., 1991; Wang et al., 2005). During such intervals, moisture migration between frontal and internal parts of the Himalaya changed, which in turn led to significantly different fluvial conditions (e.g., Bookhagen et al., 2005b; Goodbred and Kuehl, 2000; Pratt-Sitaula et al., 2004). The onset of the ISM in the early Holocene brought moisture into internal parts of the orogen where glacial deposits had been lodged since the Last Glacial Maximum and the Younger Dryas ca. 12 k.y. B.P. (e.g., Barnard et al., 2004; Owen et al., 2001). The increased moisture and resulting higher runoff likely mobilized these unconsolidated sediments and enhanced hillslope erosion to result in highly sediment-saturated rivers. The steep river gradients in the medium- to high-elevation regions support transport of these sediments. However, in the wider, low-gradient reaches of the Sutlej River, the transport capacity abruptly changes and leads to rapid deposition of excess material. This assumption is supported by our new terrace stratigraphy: (1) the clast provenance, which clearly points to a source region in the high, internal parts of the orogen and (2) the lack of cosmogenic nuclide inheritance, indicating energetic sediment removal and fast deposition. This initial deposition event is contrasted by sediment removal in the lower-elevation parts at times with a weaker ISM. In such a scenario, a decrease in sediment load after the alluviation event strengthens the river's ability to incise into the valley fill. Thus, the first terrace is inferred to (post)date the complete removal of this material during the intensified ISM in the early Holocene. Subsequently, the Sutlej River incised with ~12 mm/yr into the alluvial deposits between ca. 10 and ca. 8.7 k.y. B.P. However, during the abnormally dry ISM in-

terval starting at 8.7 k.y. B.P., less moisture reached the internal parts of the orogen. We relate this phase to reduced hillslope erosion, river discharge, and sediment load. The likely response in the fluvial system is a contraction of the channel and abandonment of a wider floodplain. This would have ultimately led to confined river incision and terrace formation as a result of changing discharge/sediment-load ratio (e.g., Bull, 1991). Similarly, the abnormally dry intervals at 6.7, 3.6, and 2.7 k.y. B.P. resulted in similar changes in the fluvial system, causing abrupt incision and hence terrace formation. However, incision rates during the early Holocene ISM were three to five times higher than late Holocene rates. This reflects the overall higher ISM rainfall in the early Holocene (e.g., Fleitmann et al., 2003; Wang et al., 2005; Dykoski et al., 2005), leading to higher runoff and thus a higher potential for fluvial incision.

Our assessment of coeval terrace cutting and periods of reduced rainfall documents two important influences of changes in moisture availability and migration on fluvial sediment flux in orogens subjected to pronounced precipitation gradients. First, the voluminous valley fill forming the substrate for the terrace surfaces in the low-gradient regions emphasizes the importance of increased precipitation as a function of moisture migration into the internal, arid, high-elevation, sectors of the orogen. The provenance of the fill material documents that these internal and high-elevation regions were the principal loci of erosion processes during the Holocene. Secondly, abnormally weak and dry ISM intervals led to a decrease in the ratio between sediment flux and transport capacity, allowing episodic incision and terrace formation, and ultimately a return to the position of the base level where it had been prior to ca. 10 k.y. B.P.

ACKNOWLEDGMENTS

We would like to thank the German Research Foundation (DFG STR371/11-1) for financial support. Discussions with D. Burbank, W. Dietrich, G. Hilley, and B. Pratt-Sitaula helped to improve an earlier version of the manuscript. Constructive and thoughtful reviews by P. Biermann, A. Heimsath, and N. Hovius helped to improve the quality of this paper. We also thank an anonymous reviewer for his insights and appreciate Bob Finkel for fast Al and Be AMS measurements.

REFERENCES CITED

Anderson, R.S., Repka, J.L., and Dick, G.S., 1996, Explicit treatment of inheritance in dating depositional surfaces using in situ Be-10 and Al-26: Geology, v. 24, p. 47–51.

Barnard, P.L., Owen, L.A., and Finkel, R.C., 2004, Style and timing of glacial and paraglacial sedimentation in a monsoon-influenced high Himalayan environment, the upper Bhagirathi Valley, Garhwal Himalaya: Sedimentary Geology, v. 165, p. 199–221.

Bookhagen, B., Thiede, R.C., and Strecker, M.R., 2005a, Abnormal monsoon years and their control on erosion and sediment flux in the high, arid northwest Himalaya: Earth and Planetary Science Letters, v. 231, p. 131–146.

Bookhagen, B., Thiede, R.C., and Strecker, M.R., 2005b, Late Quaternary intensified monsoon phases control landscape evolution in the northwest Himalaya: Geology, v. 33, p. 149–152.

Bull, W.B., 1991, Geomorphic responses to climatic change: New York, Oxford University Press, 326 p.

Burns, S.J., Matter, A., Frank, N., and Mangini, A., 1998, Speleothem-based paleoclimate record from northern Oman: Geology, v. 26, p. 499–502.

Clark, D.H., Bierman, P.R., and Larsen, P., 1995, Improving in situ cosmogenic chronometers: Quaternary Research, v. 44, p. 367–377.

Dergachev, V.A., Raspopov, O.M., van Geel, B., and Zaitseva, G.I., 2004, The ''Sterno-Etrussia'' geomagnetic excursion around 2700 BP and changes of solar activity, cosmic ray intensity, and climate: Radiocarbon, v. 46, p. 661–681.

Dykoski, C.A., Edwards, R.L., Cheng, H., Yuan, D.X., Cai, Y.J., Zhang, M.L., Lin, Y.S., Qing, J.M., An, Z.S., and Revenaugh, J., 2005, A high-resolution, absolute-dated Holocene and deglacial Asian monsoon record from Dongge Cave, China: Earth and Planetary Science Letters, v. 233, p. 71–86.

Fleitmann, D., Burns, S.J., Mudelsee, M., Neff, U., Kramers, J., Mangini, A., and Matter, A., 2003, Holocene forcing of the Indian monsoon recorded in a stalagmite from southern Oman: Science, v. 300, p. 1737–1739.

Gasse, F., Arnold, M., Fontes, J.C., Fort, M., Gibert, E., Huc, A., Li, B.Y., Li, Y.F., Lju, Q., Melieres, F., Vancampo, E., Wang, F.B., and Zhang, Q.S., 1991, A 13,000-year climate record from western Tibet: Nature, v. 353, p. 742–745.

Gasse, F., Fontes, J.C., Van Campo, E., and Wei, K., 1996, Holocene environmental changes in Bangong Co basin (western Tibet), part 4: Discussion and conclusions: Palaeogeography, Palaeoclimatology, Palaeoecology, v. 120, p. 79–92.

Goodbred, S.L., and Kuehl, S.A., 2000, Enormous Ganges-Brahmaputra sediment discharge during strengthened early Holocene monsoon: Geology, v. 28, p. 1083–1086.

Granger, D.E., and Smith, A.L., 2000, Dating buried sediments using radioactive decay and muogenic production of Al-26 and Be-10: Nuclear Instruments and Methods in Physics Research B, v. 72, p. 822–826.

Grootes, P.M., Stuiver, M., White, J.W.C., Johnson, S., and Jouzel, J., 1993, Comparison of oxygen isotope records from the GISP2 and GRIP Greenland ice cores: Nature, v. 366, p. 552–554.

Gupta, A.K., Anderson, D.M., and Overpeck, J.T., 2003, Abrupt changes in the Asian southwest monsoon during the Holocene and their links to the North Atlantic Ocean: Nature, v. 421, p. 354–357.

Kohl, C.P., and Nishiizumi, K., 1992, Chemical isolation of quartz for measurement of in situ-produced cosmogenic nuclides: Geochimica et Cosmochimica Acta, v. 56, p. 3583–3587.

Lachniet, M.S., Asmerom, Y., Burns, S.J., Patterson, W.P., Polyak, V.J., and Seltzer, G.O., 2004, Tropical response to the 8200 yr BP cold event? Speleothem isotopes indicate a weakened early Holocene monsoon in Costa Rica: Geology, v. 32, p. 957–960.

Lal, D., 1991, Cosmic-ray labeling of erosion surfaces—In situ nuclide production rates and erosion models: Earth and Planetary Science Letters, v. 104, p. 424–439.

Lister, G.S., Kelts, K., Zao, C.K., Yu, J.Q., and Niessen, F., 1991, Lake Qinghai, China—Closed-basin lake levels and the oxygen isotope record for Ostracoda since the latest Pleistocene: Palaeogeography, Palaeoclimatology, Palaeoecology, v. 84, p. 141–162.

Nishiizumi, K., Winterer, E.L., Kohl, C.P., Klein, J., Middleton, R., Lal, D., and Arnold, J.R., 1989, Cosmic-ray production rates of Be-10 and Al-26 in quartz from glacially polished rocks: Journal of Geophysical Research Solid Earth and Planets, v. 94, p. 17,907–17,915.

Ohno, M., and Hamano, Y., 1992, Geomagnetic poles over the past 10,000 years: Geophysical Research Letters, v. 19, p. 1715–1718.

Owen, L.A., Gualtieri, L., Finkel, R.C., Caffee, M.W., Benn, D.I., and Sharma, M.C., 2001, Cosmogenic radionuclide dating of glacial landforms in the Lahul Himalaya, northern India: Defining the timing of late Quaternary glaciation: Journal of Quaternary Science, v. 16, p. 555–563.

Pratt-Sitaula, B., Burbank, D.W., Heimsath, A., and Qjha, T., 2004, Landscape disequilibrium on 1000–10,000 year scales Marsyandi River, Nepal, central Himalaya: Geomorphology, v. 58, p. 223–241.

Repka, J.L., Anderson, R.S., and Finkel, R.C., 1997, Cosmogenic dating of fluvial terraces, Fremont River, Utah: Earth and Planetary Science Letters, v. 152, p. 59–73.

Rohling, E.J., and Pälike, H., 2005, Centennial-scale climate cooling with a sudden cold event around 8200 years ago: Nature, v. 434, p. 975–979.

Stuiver, M., Reimer, P.J., Bard, E., Beck, J.W., Burr, G.S., Hughen, K.A., Kromer, B., McCormac, G., Van der Plicht, J., and Spurk, M., 1998, INTCAL98 radiocarbon age calibration, 24,000–0 cal BP: Radiocarbon, v. 40, p. 1041–1083.

Thompson, L.G., Yao, T., Mosley-Thompson, E., Davis, M.E., Henderson, K.A., and Lin, P.N., 2000, A high-resolution millennial record of the South Asian monsoon from Himalayan ice cores: Science, v. 289, p. 1916–1919.

Van Campo, E., Cour, P., and Sixuan, H., 1996, Holocene environmental changes in Bangong Co basin (western Tibet), part 2: The pollen record: Palaeogeography, Palaeoclimatology, Palaeoecology, v. 120, p. 49–63.

Wang, Y.J., Cheng, H., Edwards, R.L., He, Y.Q., Kong, X.G., An, Z.S., Wu, J.Y., Kelly, M.J., Dykoski, C.A., and Li, X.D., 2005, The Holocene Asian monsoon: Links to solar changes and North Atlantic climate: Science, v. 308, p. 854–857.

Manuscript received 8 February 2006
Revised manuscript received 23 February 2006
Manuscript accepted 28 February 2006

Printed in USA